Combined experimental and numerical study on micro-cube indentation splitting test of cement paste

Zhang, Hongzhi; Šavija, Branko; Schlangen, Erik

DOI
10.1016/j.engfracmech.2018.04.018

Publication date
2018

Document Version
Final published version

Published in
Engineering Fracture Mechanics

Citation (APA)
Zhang, H., Šavija, B., & Schlangen, E. (2018). Combined experimental and numerical study on micro-cube indentation splitting test of cement paste. *Engineering Fracture Mechanics*, *199*, 773-786. https://doi.org/10.1016/j.engfracmech.2018.04.018

Engineering Fracture Mechanics 199 (2018) 773–786

Contents lists available at ScienceDirect

Engineering Fracture Mechanics

journal homepage: www.elsevier.com/locate/engfracmech

Combined experimental and numerical study on micro-cube indentation splitting test of cement paste

Hongzhi Zhang*, Branko Šavija, Erik Schlangen

Microlab, Faculty of Civil Engineering and Geosciences, Delft University of Technology, Delft 2628 CN, The Netherlands

ARTICLE INFO

Keywords:
Micromechanics
Splitting tensile strength
Micro-cube splitting
Lattice modelling
Cement paste

ABSTRACT

The aim of this paper is to investigate the fracture performance of cement paste at micro scale by both experimental and numerical methods. Micro cubic specimens with length of 100 μm were fabricated by precision cutting, grinding and micro-dicing, and tested by splitting with a wedge tip mounted on a nano-indenter. A nominal splitting tensile strength was derived from the maximum load of the recorded load-displacement diagram to represent the global fracture performance of the fractured micro-cube. To achieve this, an analogy was made between the micro-cube indentation splitting test and the standard Brazilian splitting test. To cope with the inherent heterogeneity of this material at micro scale, for cement paste with each water/cement (w/c) ratio (0.3, 0.4 and 0.5), more than hundred micro-cube specimens were fabricated, tested and analysed using Weibull statistics. The analysis shows that the splitting tensile strength of cement paste on the micro scale is much higher than on the macroscopic scale but lower than tensile strength of distinct hydrated cement phases measured on micro or nano scale. Furthermore, higher and less scattered values of splitting tensile strength were observed for the specimens with lower w/c ratio. In parallel with the experiments, a micro-structure informed lattice fracture model was adopted to simulate the fracture process of the micro-cube under indentation splitting. The simulated results were compared with the experimental one and have a good consistency in terms of the load-displacement curve and fracture pattern. With the method presented in this paper the framework for validation of the modelling results at micro scale is created.

1. Introduction

Concrete is a material with heterogeneities at length scales ranging from sub-nanometres to metres, and its mechanical properties are affected by various factors at all composite scales [1]. To cope with its multi-scale nature, multi-scale strategies are commonly applied [2–6]. At the μm scale the internal structure of hardened cement paste is the most important structural feature, comprising various phases, i.e. the hydration products (inner hydration product, outer hydration product and calcium hydroxide) [7], anhydrous cement particles and capillary pores. At higher (cm) scale, cement paste is homogenized together with the aggregates and the interfacial transition zone between these two phases, while at lower scale distinct hydration products containing nano pores and capillary pores are regarded as the study objects. To properly understand the fracture performance and predict the mechanical properties of such material, experiments and simulations need to be carried out at each length scale.

Recent studies, both experiments and simulations, found that the tensile strength of components in cement paste at micro scale is much higher than the macroscopic value of concrete (a few MPa). For example, in molecular dynamics models, tensile strength of

* Corresponding author.
E-mail addresses: h.zhang-5@tudelft.nl (H. Zhang), b.savija@tudelft.nl (B. Šavija), erik.schlangen@tudelft.nl (E. Schlangen).

https://doi.org/10.1016/j.engfracmech.2018.04.018
Received 1 February 2018; Received in revised form 9 April 2018; Accepted 12 April 2018
Available online 13 April 2018
0013-7944/

pure C-S-H globules is predicted from 1 GPa to 3 GPa depending on dry or wet conditions [8], while low and high density C-S-H phases are predicted to have tensile strengths of 66 MPa and 320 MPa, respectively, by means of inverse analysis using a multi-scale model [3]. In addition, micro-cantilever experimental measurements (length scale of several μm) show that the tensile strengths are around 264 MPa, 700 MPa and 655 MPa for outer products, inner hydration products, and calcium hydroxide, respectively [9]. Therefore, it is expected that the studies on cement paste at micro scale could fill the gap between nano scale and meso scale.

However, due to the technical and instrumental demands, studies at this level are mostly carried out by simulations [2,6,10–15]. In the micro scale simulations, material microstructure and local mechanical properties are considered as the most important issues. The microstructure can be obtained by numerical models (e.g. HYMOSTRUC [16], CEMHYD3D [17] and μic [18]) or by experimental methods (e.g. environmental scanning electron microscopy (ESEM) [19] and X-ray microcomputed tomography (XCT) [20]). However, the input local mechanical properties for different phases and the bonding between them are always debated, since these values are expected to be measured experimentally. While nanoindentation can be considered appropriate for measuring the elastic properties of cement paste and its individual phases, more complex procedures are needed for measuring strength properties at the micro scale. This is because no relation between the indentation hardness and strength has been found so far for cement based materials [13,21]. Therefore, more advanced procedures that use e.g., nano-indentation equipment need to be used to measure the strength or provide the experimental observation which can be used for calibrating and validating the micro scale simulation.

Recently, micro-cantilever bending tests have been proposed to measure the tensile strength of cement paste [22] and it's individual phases [9]. This technique involves milling of a cantilever beam in the material using focused ions, typically in the size range of up to 10 μm. Such specimen is subsequently loaded in bending and tested until failure, providing a measure of the elastic modulus and the flexural strength of the tested volume. A major drawback of this approach is the time-consuming specimen preparation, which typically results in a relatively small number of specimens tested. One should keep in mind that on the micrometre length scale high scatter of measured mechanical properties can be expected [23,24] and that a large number of tests need to be performed for the measurements to be statistically reliable. Herein a different approach is proposed.

In this study, a precision micro-dicing technique is adopted for micro scale specimen preparation. In this way, a large number of micro-cubes can be fabricated in a short period of time [21]. In this study, these cubes were split by applying a line force at centre of the top surface using a wedge tip mounted on a nanoindenter. Splitting tensile strength was then derived from the recorded maximum load using an analogy with the analytical solution of a classic Brazilian splitting test. Hardened cement pastes with different w/c ratios (0.3, 0.4 and 0.5) were investigated. Considering the heterogeneous nature of this material at micro scale, at least one hundred specimens for each w/c ratio were tested and the so-called Weibull statistics was adopted to conduct the statistical analysis of measured strength.

In addition to the experiments, a microstructure informed lattice fracture model was used to study the fracture process of the micro-cube under the indentation splitting. Such fracture model requires digitalized microstructure and mechanical properties of induvial phases. The input mechanical properties of individual phases are calibrated by the authors [21] using the experimental data from where the same size micro-cube was fractured by a Berkovich tip. It is therefore expected that a validation procedure can be conducted in the current work by conducting different boundary conditions on the micro-cube and compared with the experimental results. In this way, an integrated system for fitting and validating micro scale fracture simulation can be completed.

2. Experimental details

2.1. Materials and micro-cube preparation

Standard grade OPC CEM I 42.5 N cement and deionized water were used in this study. The w/c ratios of pastes were 0.3, 0.4 and 0.5. After 1 min of mixing at low speed and two minutes mixing at high speed, the fresh mixtures were poured into a cylindrical bottle with 24 mm diameter and 39 mm height. The pastes were carefully compacted on a vibrating table to release entrapped air and then sealed with a plastic lid. In order to minimize bleeding, the samples were rotated at a speed of 2.5 rpm at room temperature (20 °C) for 24 h. After 28 days curing period in sealed conditions at room temperature, specimens were demoulded and cut into 2 mm thick slices. Before testing, hydration of these slices was terminated using isopropanol [25].

The slice was bound on the objective glass and ground down to 100 μm with a Struers thin section system. For purpose of grinding, a diamond ring grinding disc which has grit size of 35 μm was used. To ensure that both surfaces of the produced slice are flat, the specimen was first ground down to 1 mm and then turned around to continue the grinding procedure until the required thickness was reached. After grinding, samples were polished with 6 μm (5 min), 3 μm (5 min), 1 μm (10 min), and 0.25 μm (30 min) diamond paste on a lapping table. After each polishing step, samples were soaked into an ultrasonic bath to remove any residue. Sample preparation was performed just prior to testing to avoid carbonation of the tested surface. Afterwards, to fabricate the micro-cubes from the slice, a micro dicing saw (MicroAce Series 3 Dicing Saw, mainly applied for semiconductor wafers cutting) was used to cut through the slice over two mutually perpendicular directions as schematically shown in Fig. 1. In order to make sure that the cement paste cubes have the required dimensions and that the adhesive between the cement paste and the glass is sliced, the blade was set to cut a few micrometres into the glass plate. An environmental scanning electron microscope (ESEM) was then used to observe the produced micro-cube arrays (Fig. 2a) and check the geometry information of each cube as shown in Fig. 2b. The final cubes are all with a dimension of $100 \times 100 \times 100 \pm 3\,\mu m$.

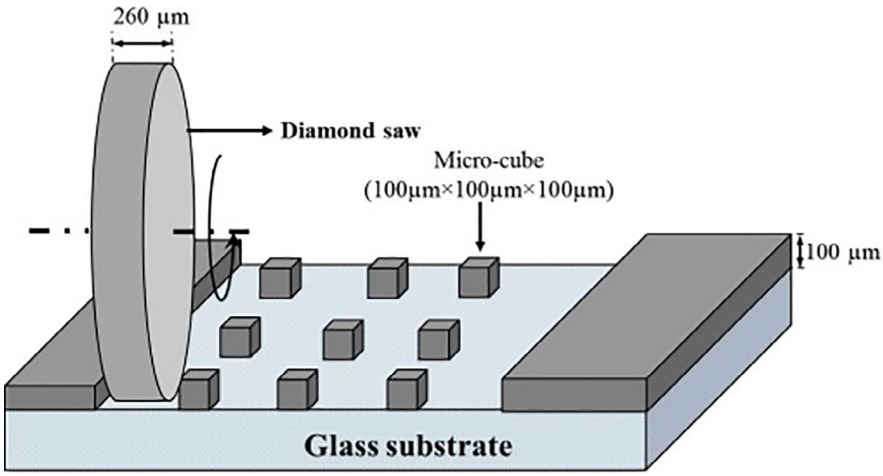

Fig. 1. Schematic illustration of micro-cube arrays fabrication using micro dicing saw.

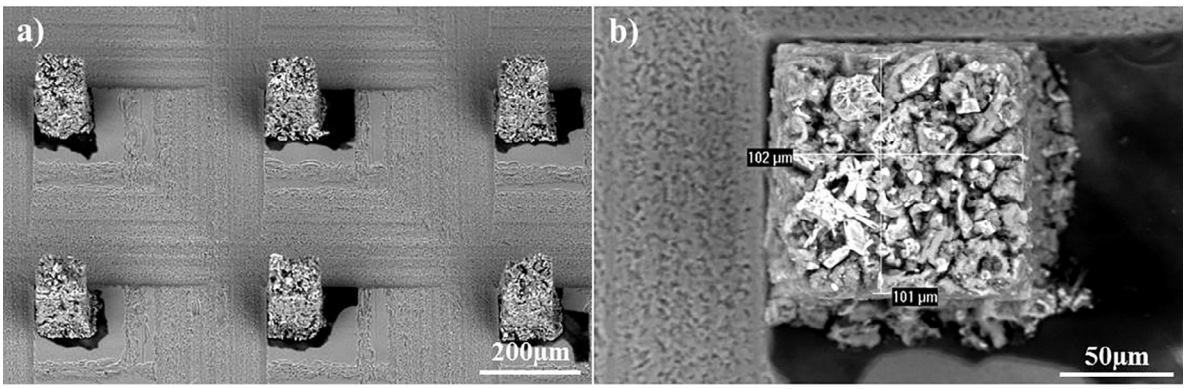

Fig. 2. (a) micro-cube arrays on the glass substrate. (b) Top view of a single cube with dimensions, showing visible porosity.

2.2. Micro-cube indentation splitting test

The micro-cube splitting test is conducted by applying a line load at the centre on top surface of the specimen as schematically shown in Fig. 3, which was achieved by an Agilent G200 nano-indenter equipped with a diamond wedge indenter tip (Fig. 4). Length and radius of the cylindrical edge are 200 µm and 9.6 µm, respectively. The micro-cube was progressively loaded with a constant displacement increment of 50 nm/s until failure. Force and displacement data were acquired using the continuous stiffness

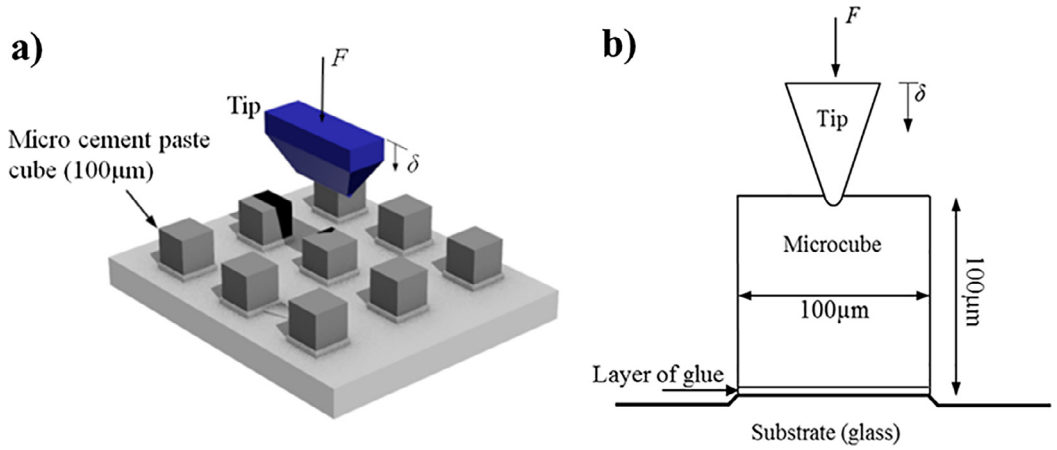

Fig. 3. Schematic illustration of (a) the micro-cube splitting procedure. (b) The contact mechanics between indenter tip, micro-cube and substrate.

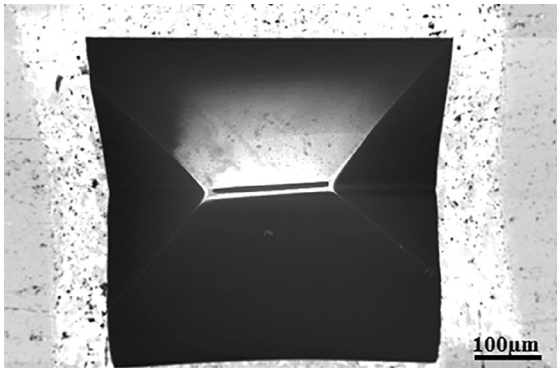

Fig. 4. Top view of the diamond wedge tip with 200 μm in length and a round apex with a radius of 9.6 μm.

measurement (CSM) technique [26] and the applied CSM settings are: 2 nm amplitude, 45 Hz frequency and 100 N/m surface detection. The maximum load capacity of the instrumented nano-indenter is around 635 mN. It should be noted that the stiffness or modulus of tested micro-cubes cannot directly be obtained from the recorded load-displacement curves, because the measured displacement includes the deformation of the supporting adhesive-layer and local imprinting of the indenter into the micro-cube. This influence is further studied by the lattice fracture simulation, as shown later. A typical load-displacement curve recorded by the nano-indenter is shown in Fig. 5. Clearly two regimes as well as the maximum load point at failure stage can be distinguished from this curve. In regime (I), the load on sample increases monotonically until reaching the critical splitting load (maximum load) P_u. Once the load exceeds P_u, the system transitions from a stable regime (I) towards an unstable regime (II). The horizontal line in regime (II) indicates an overshoot behaviour of the wedge indenter tip towards the substrate because of the structural collapse of the micro-cube. Since displacement control of the nano-indenter is not fast enough, it is not possible at present to capture the post-peak behaviour of the specimen. Furthermore, the behaviour might be brittle, and the system cannot capture a snap-back.

Additionally, in order to visually observe the fracture mechanism of this test, different loading depths were applied. After test, the fractured specimens were examined using ESEM and the micrographs are presented in Fig. 6. Since the indented specimen is small enough, the structural damage occurs under a relatively low force and the typical failure mechanism is splitting of the material in which the main cracks extend and propagate under the tip until the specimen is split in two halves across the plane of loading.

2.3. Splitting tensile strength assessment using FEM

As a structural collapse happens to the micro-cube once a critical load is reached during testing, a parameter (i.e. strength) that could represent the global mechanical performance can be derived from the critical load. This enables a quantitative study of the micromechanical performance. Since the boundary conditions of micro-cube splitting test are similar to a standard Brazilian splitting test (NEN-EN 12390-6 Standard) for splitting tensile strength assessment of cement based materials, it is expected that the tensile stress can be predicted in a similar way. An analogy between these two tests was made to achieve this by assessing the stress distributions of specimens under corresponding loading conditions using linear elastic, homogeneous, and isotropic finite element modelling (FEM). It has to be noted that, although the micro-cube paste specimens clearly cannot be considered as homogeneous and

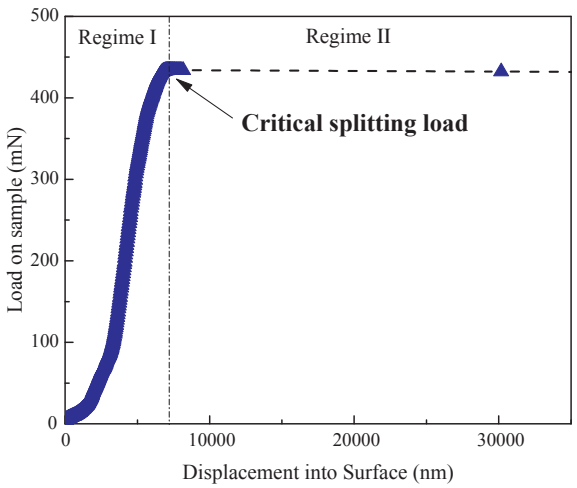

Fig. 5. A typical load versus displacement response measured in the micro-cube splitting test.

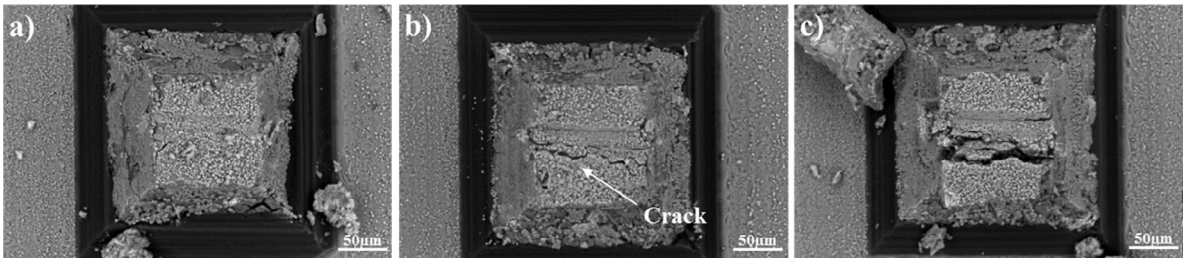

Fig. 6. Three stages in the micro-cube splitting process: (a) initial stage of the loading; (b) crack starts to propagate next to the tip; (c) splitting failure of the micro-cube.

isotropic on this length scale, these assumptions were made in order to enable a relatively simple conversion of measured values to splitting strength by comparing it to a standard test (i.e. the Brazilian test). The influence of heterogeneity in the mechanical behaviour of paste on this length scale is discussed later.

In the Brazilian test, a pair of symmetrical line loads are applied by compressing two parallel bearing strips at the centre of both top and bottom surfaces of cubic specimen, as schematically shown in Fig. 7. This geometry and loading conditions lead to a nearly uniform tensile stress state in the central plane of the specimen and the stress becomes more uniform as the strips become narrower. Therefore, the expected failure mode of this test is the split of specimens in two halves (similar to the observation in micro-cube splitting test). According to elastic theory the maximum stress is a measure of the splitting tensile strength which is defined as [27,28]:

$$f_{st} = \frac{2P}{\pi D^2} \tag{1}$$

where P is the maximum load, D is the length of cube. Simultaneously, a commercial FEM software package Femmasse was used for simulation of stress distribution in which materials properties were set as homogeneous, isotropic, and linear elastic. For simplicity, only half of the specimen with 50 × 100 FE grid mesh was simulated. The loading was simplified as a concentred point load and a vertical displacement support at symmetry axis as shown in Fig. 8a. Fig. 8b presents the simulated contours of equal principal tensile stress. Clearly the numerical simulated maximum stress is consistent with the analytical solution in Eq. (1). Afterwards, the numerical modelling for micro-cube splitting was achieved by clamping the bottom surface as shown in Fig. 9a, while other parameters remained unchanged. The results are shown in Fig. 9b. It is found that the maximum tensile stress for both simulations appears in the central plane and the ratio between micro-cube splitting and Brazilian splitting is around 0.73. Although the tension zone is smaller and moved upwards, it is expected that to break the same brittle-elastic specimen the Brazilian test needs 0.73 load of the micro-cube splitting test. Therefore, a reduction factor $\alpha = 0.73$ is added in Eq. (1) to derive the splitting tensile strength from measured

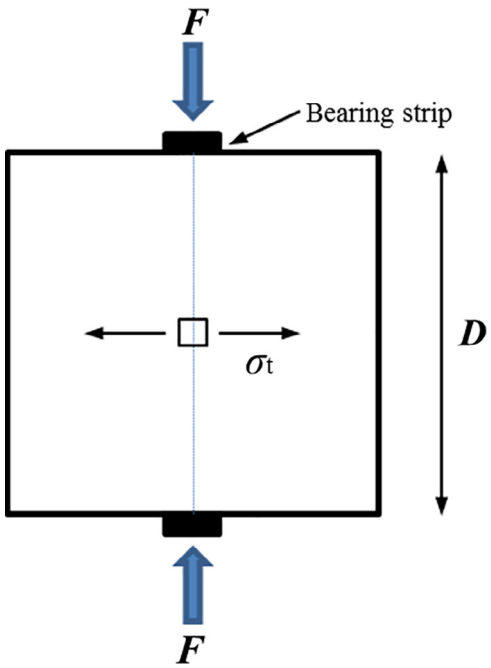

Fig. 7. Load configuration of Brazilian test on cubic specimen.

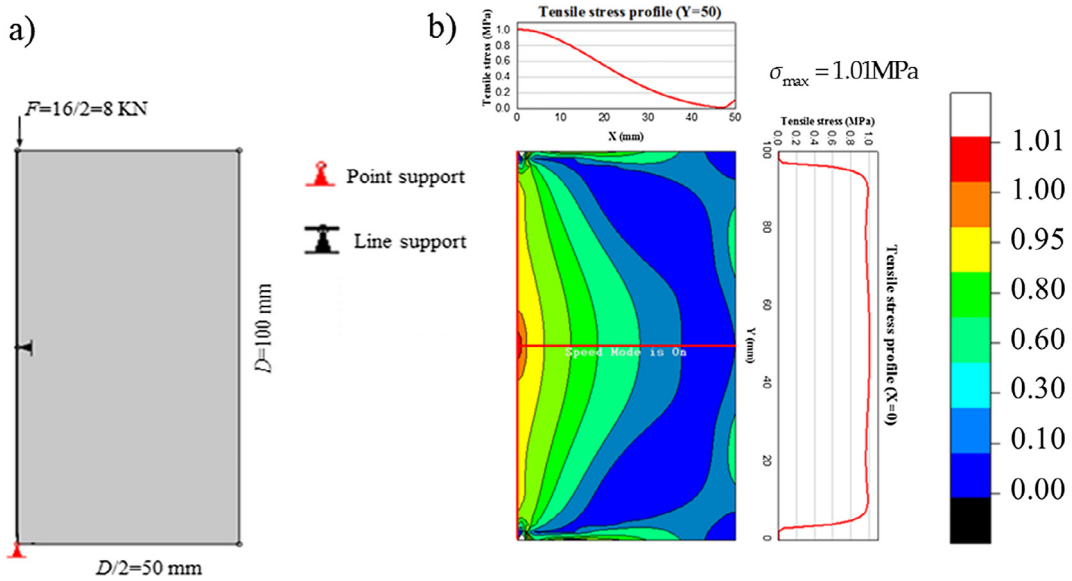

Fig. 8. 2D FEM computations of Brazilian test: (a) Boundary conditions. (b) Contours of equal principal tensile stress.

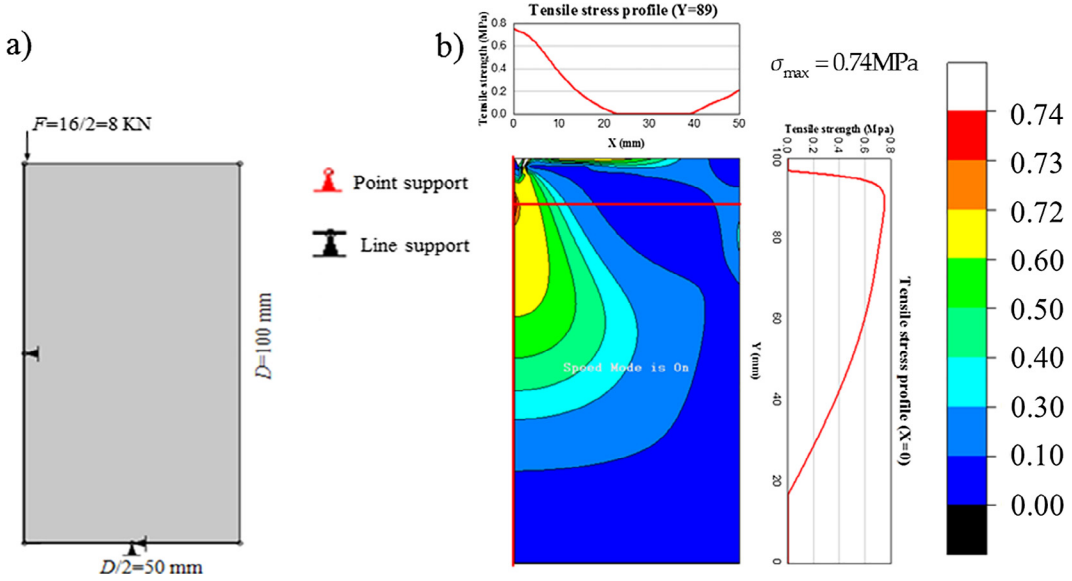

Fig. 9. 2D FEM computations of micro-cube splitting test: (a) Boundary conditions. (b) Contours of equal principal tensile stress.

maximum load in the current test:

$$f_{st} = \alpha \frac{2P_u}{\pi D^2} \tag{2}$$

Eq. (2) was therefore used to convert the maximum load to splitting strength in the following sections.

3. Fracture modelling

3.1. Digital micro cement paste cube

Digital cubic specimens with a size of 100 μm (Fig. 10, same size with the real specimen) were generated by a XCT technique as described in [21]. Firstly, a cement paste prism having a cross-section of 400 μm × 400 μm was made from a 28-day cured cylindrical sample with initial w/c ratio of 0.4 (height: 39 mm and diameter:24 mm) by cutting, polishing and micro-dicing. This prism was scanned with a CT-scanner to obtain the high resolution (2 μm^3/voxel) greyscale images. Then, a so-called global threshold method

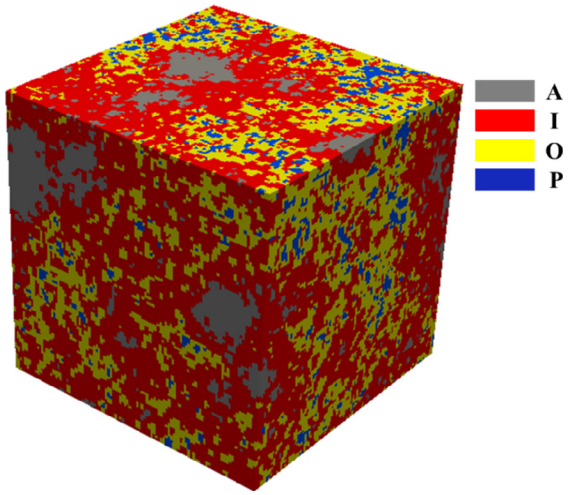

Fig. 10. Microstructure of cement paste with w/c 0.4 and size 100 μm × 100 μm × 100 μm at the curing age 28 days from XCT experiments [21].

[19,20,29,30] was chosen to segment the greyscale images into four phases, namely, anhydrous cement grains (A), inner (I) and outer (O) hydration products and pores (P). The total porosity and hydration degree were regarded as 11.84% and 74.99% respectively according to the segmented images. Limited by the current resolution, capillary pores smaller than 2 μm and gel pores are not detectable. Although it is reported that these pores have a significant influence on the mechanical properties, especially at early age [6,14], the main aim of current simulation is to offer more insights into the fracture process of the micro-cube under indentation splitting and use the recorded load-displacement curve as validation of the predicted micromechanical properties, therefore influence of microstructure at lower scale (smaller than the current resolution) is not taken into account. In order to show the stochastic micromechanical properties of cement paste, 10 cubes were randomly extracted from different locations and investigated using the discrete lattice fracture model.

3.2. Model description

Discrete lattice fracture model can be utilized for modelling the fracture process of quasi-brittle material. e.g. cement-based material [13,31] and graphite [24,32]. In the lattice model, the material is discretized by a set of beam elements having linear elastic behaviour (i.e. strength and elasticity). Firstly, inside each voxel of the digital specimen, one node was randomly positioned and Delaunay triangulation was performed, as described in [33], to determine the connectivity of a set of nodes. Then, a set of linear elastic analyses is performed by calculating the nodal responses of the lattice network for an external boundary displacement. With the current discretization, a lattice system with 50 × 50 × 50 nodes and 937,247 elements was generated and the mesh configuration that is chosen results in a Poisson's ratio of about 0.18. At every analysis step, a displacement is applied, a critical beam element with the highest stress/strength ratio is labelled and removed from the mesh, thereby introducing a small crack. In the present work, a fracture criterion considering both normal force and bending moments in beam elements is adopted:

$$\sigma = \alpha_N \frac{N}{A} + \alpha_M \frac{\max(M_X, M_Y)}{W} \tag{3}$$

where A is the beam cross-sectional area, W the cross-sectional moment of resistance. α_N and α_M are the normal force influence factor and the bending influence factor. Their values are most commonly adopted as 1.0 and 0.05, respectively [34]. These values have also been adopted herein. This procedure is then repeated with the updated geometry and stiffness of the whole lattice network until structural failure happens. As a consequence, the fracture pattern of the investigated material volume at each step can be obtained as well as their load-displacement response which can be further compared to the laboratory observed load-displacement diagram of the specimen under loading.

The heterogeneity is achieved by assigning different properties to the beams according to the digital material structure obtained by XCT technique. The mechanical properties of beam elements (elasticity modulus and strength) depend on the phase type of connected two voxels. Three solid phases in the microstructure result in six types of lattice elements as shown in Fig. 11. Elasticity modulus of beam element was ascribed with the harmonic average of the connected two phases, while the strength assigned as the lower value in between. The mechanical parameters of each single phase used in this study are presented in Table 1. Elastic moduli are assumed equal to the nanoindentation measurements for individual phases in cement paste matrix [35]. The tensile strengths are taken from a previous study by the authors [21], wherein a micro scale experiment is developed to calibrate these values. In the current study, the elements are allowed to fail in the compression state as well. The compressive strength of each phase is estimated 20 times as high as its tensile strength. Note that a lower elastic modulus of anhydrous cement grain is reported in [35] compared with the value reported by Velez et al. [36] on synthesized pure clinker phases and adopted in this study. This is because the residual

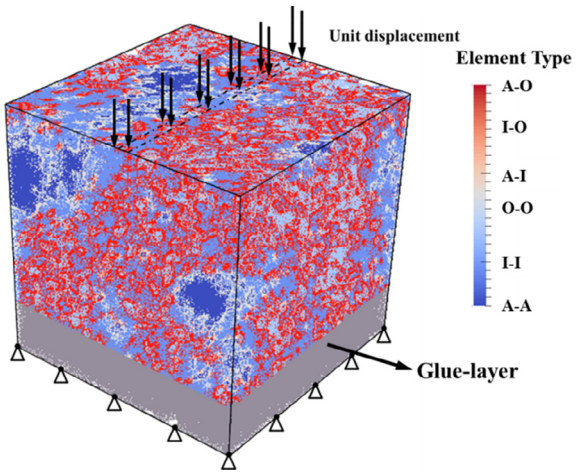

Fig. 11. Fracture modelling of micro-cube under indentation splitting.

Table 1
Assigned local mechanical properties of individual phases at micro scale [21].

Phase	Young's modulus (GPa)	Strength (MPa)
Anhydrous cement	99	683
Inner product	31	92
Outer product	25	58

cement particles in hydrated cement pastes are more porous [37].

In terms of the boundary conditions, the nodes at bottom surface were clamped to represent the glued sample on the glass plate. A vertical displacement was applied on nodes in the two lines closed to the middle axis of the top surface to mimic the indenter load. It is emphasized that in order to show a more realistic elastic fracture behaviour of micro cube under indentation, the lattice elements (coloured grey in figure) located up to 20 μm from the bottom were set as adhesive element with a low elastic modulus of 3 GPa (measured by a grid nano-indentation test as stated in Appendix A) to represent the adhesive layer between cement paste and glass substrate. The glue layer was set to be linear elastic.

4. Results and discussion

4.1. Experimental results and discussion

For each w/c ratio, at least one hundred micro-cube specimens were fabricated and tested. Histograms of measured splitting tensile strengths are shown in Fig. 12. The results exhibit a great dispersion owing to the heterogeneous nature of the material at this scale. Thus, it is preferable to analyse the experimental data by Weibull statistics. For samples which have the same volume, the probability of fracture P_f can be written as [38]:

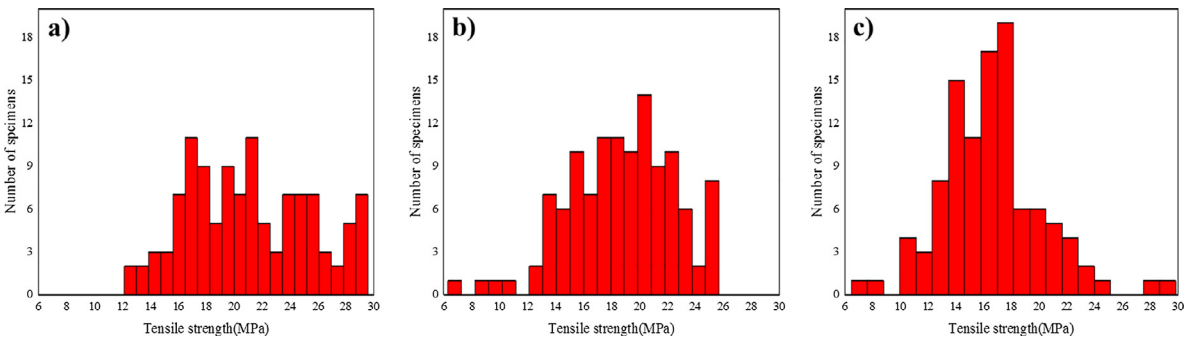

Fig. 12. Measured splitting tensile strength of cement paste micro-cubes with different w/c ratios: (a) 0.3, (b) 0.4 and (c) 0.5.

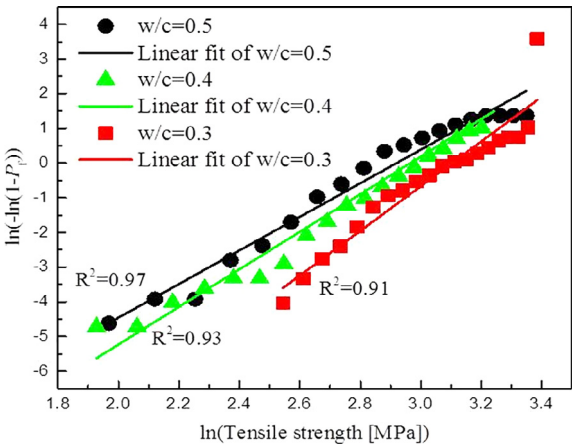

Fig. 13. Weibull plot for measured splitting tensile strength of cement paste micro-cubes with different w/c ratios.

$$P_f = 1-\exp\left[-\left(\frac{\sigma}{\sigma_0}\right)^m\right] \tag{4}$$

where m is the Weibull modulus and σ_0 is the stress corresponding to 63% probability of fracture, also known as the scaling parameter. Fig. 13 displays plots for the splitting tensile strength tests for the 3 cement paste specimens with w/c ratio 0.3, 0.4 and 0.5 in a Weibull coordinate. Although some deviation from the best-fit line occurred at the high strength extreme of cement paste with a w/c ratio of 0.3, a reasonable agreement is demonstrated between the best straight-line fit and the experimental data points with a high coefficient of determination (R^2). This difference is introduced because of the limited load capacity of the instrumented nano-indenter, which is around 635 mN corresponding to a strength limitation of 29.5 MPa. Once the response of the load reached this value, the test was stopped, and this value was recorded as the maximum load leading to a sharp increase of the cumulative probability at the high strength extreme.

For the 3 tested materials, the Weibull modulus and scaling parameter were fitted using the least squares method and summarized in Table 2. It shows that m and σ_0 increase with the decrease of w/c ratio of the cement pastes. It indicates that the cement paste with a lower w/c ratio yields a higher fracture strength and less varying mechanical properties. This can be mainly explained by the decreased volume and varied size distribution of capillary pores in specimens where the capillary pore works as the initial defect and introduce local stress concentration upon loading [39]. Similar observations are also reported in concrete at a higher scale [40].

The present work has, for the first time, shown the values of stochastic tensile strength of cement paste at micro scale. These values are much higher than the macroscopic values of cement paste or concrete and one order of magnitude lower than the microscopic values of distinct hydrated cement phases [9]. This agrees with the scaling law of quasi-brittle material in which theoretical strength increases as the sample size or scale decreases [41], and indicates that different levels defects exist in cement based materials: on one hand capillary pores would have a large effect on the decrease of strength at micro scale and on the other hand unavoidable micro-cracks, large capillary pores and entrapped air voids introduce decrease on strength at a upper scale [1]. To the author's best knowledge, the only other reported experimental tensile strength of cement paste at this scale is from measurements of a single FIB machined micro-cantilever with rhomboidal cross section (3.5 μm in with, 5 μm in length) and identified to be 2.67 MPa [22], which is in contradiction to scaling law of strength to micrometres in quasi-brittle materials [41]. Furthermore, the Young's modulus of these tested micro-cantilever is reproduced from the recorded load-displacement curve and seems to be unrealistically low (less than 0.13 GPa). Therefore, it is not possible to use this test as a baseline for comparison. Furthermore, it is worth mentioning that a statistical distribution of mechanical properties should be provided by the modelling instead of deterministic value due to the inherent heterogeneous microstructure and quasi-brittle properties of this material. This could be done by means of an e.g. random fields model [42].

It is emphasized that, although the way to derive the nominal splitting strength considers the material as the perfect isotropic elastic material, the aim of this method is to set a proper parameter which can be used to represent the global mechanical properties of the tested material, so that the influence of the change of the microstructure on the yield strength at this scale can be quantified and compared to each other. In the current research, we showed the influence of initial w/c ratio on the micromechanical properties

Table 2
Weibull parameters for the measured splitting tensile strength.

w/c ratio	Number of specimens	m	σ_0 (MPa)	Mean values ± standard deviation (MPa)
0.3	115	6.45	22.27	21.28 ± 4.29
0.4	117	5.14	19.48	18.72 ± 3.85
0.5	105	4.86	18.54	16.54 ± 3.71

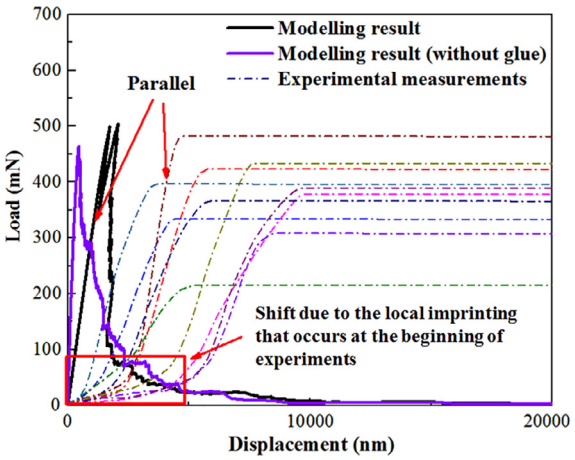

Fig. 14. Comparison between the simulated load-displacement curve of micro-cube under indentation splitting.

and it is expected that the influence of other factors, i.e. hydration time and degradation on the micromechanical properties can be investigated quantitatively by the method proposed in this study.

4.2. Numerical results and discussion

Fig. 14 presents the comparison between simulated load-displacement curves of one micro-cube under indentation splitting and those measured experimentally (dot lines). For comparison, the experimental load-displacement curve of 10 specimens were plotted. As state above, the horizontal line represents the overshoot behaviour of the indenter. The influence of adhesive-layer on the fracture performance of cement paste is investigated by comparing the simulations with and without the adhesive-layer. As the post-peak behaviour cannot be captured experimentally at present, only the ascending branch was used for the comparison. Clearly, the simulation considering the adhesive-layer has a good agreement with the experimentally measured curves in terms of the maximum load and slope of load-displacement curve (stiffness). Due to the fact that a local imprinting of the indenter into the micro-cube occurs at the beginning of the experiments, the measurements are slightly shifted, but the slope remains similar to the one in simulated load displacement curve. In addition, it can be seen from the simulation that the stiffness is significantly decreased by adding the adhesive-layer at the bottom, while the peak load is slightly increased. It is also clear that, in the simulations, a post peak response can be observed, which is impossible to observe in the experiment due to limitations of the equipment described previously. Note that the behaviour in the simulation with glue layer is brittle with several snap-backs. This can be captured by the model, but not in the experiments. As this is one of the first attempts at directly testing cement paste specimens at the micrometre length scale, this is not seen as a problem at the moment. In fact, it should be noted that, even on the macro-scale, observing of the post-peak behaviour remains a challenge for certain types of materials, and for such cases it is also necessary to design specific test setups [43]. The simulated crack pattern of these two cases corresponding to the peak load point are compared in Fig. 15. It is evident that, in both cases, the micro-cube was split in half as the maximum tensile stress always exists in the middle axis below the tip, although some local cracks are observed along the tip edge and around defects (pores) because of the stress concentration, which is in accordance with the experimental observation as shown in Fig. 6. Furthermore, it is observed that a straighter vertical main crack exists in the micro-cube without adhesive layer, while the crack pattern in the simulation considering the adhesive layer is more inclined to one side because of the bottom is confined by the adhesive layer. Therefore, a higher load capacity is expected for the one with the adhesive layer.

It is emphasized that the input mechanical properties of individual phases in cement (e.g. anhydrous cement, inner hydration products and outer hydration products) are calibrated by the authors [21] using experimental data from where the same size micro-cubes were fractured by a Berkovich tip using nano-indenter. It is showed that these input local mechanical properties can be applied to lattice fracture simulations under different boundary conditions and have satisfactory results. Together with the method presented in [21] the framework for fitting and validation of the modelling results at micro scale is created.

The crack patterns at different test stages are plotted in Fig. 16. It shows that the crack first initiates around the tip and the middle axis beneath the tip. After localising, a relatively straight vertical crack forms in the upper part and propagates to the bottom and turns to lean to the right-hand side because of the adhesive layer.

It should be kept in mind that the test results show a high variability which is introduced by the inherent heterogeneity of this material at this length scale. Therefore, multiple voxel-based digital specimens were generated and tested. The simulated load-displacement curves are shown in Fig. 17. Clearly, the stochastic nature of the mechanical properties can be successfully reproduced numerically by choosing the same size volume ($100 \times 100 \times 100\ \mu m^3$) from different locations in the XCT characterised material structure. The average nominal splitting strength of these 10 cubes is 21.43 MPa which slightly higher than the experimentally measured value (18.72 MPa). This can be attributed to the deviation of the statistics as the number of the investigated digital specimens might not be large enough to represent the stochastic nature of cement paste at this scale. However, the number of

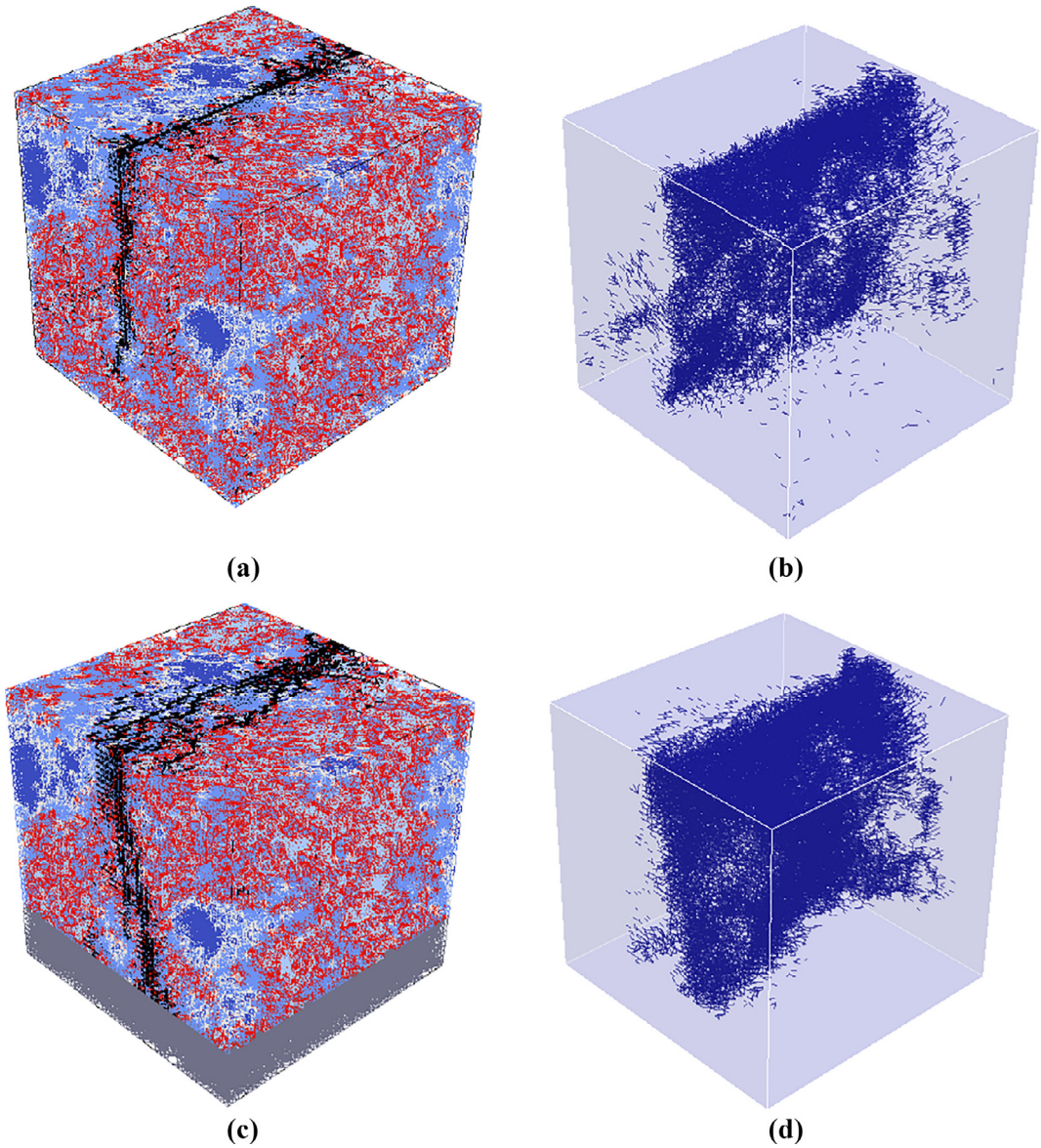

Fig. 15. Simulated crack pattern of one cement paste micro-cube under indentation splitting: (a) showing the microstructural features, without the glue layer; (b) showing only the crack, without the glue layer; (c) showing the microstructural features, with the glue layer; (d) showing only the crack, with the glue layer.

simulations was limited due to the large computational efforts. Nevertheless, as simulation requires detailed material information from where porosity can be obtained, the strength-porosity relationship was studied. Fig. 18 presents the correlation relationship between the predicted splitting strength and porosity. It is found that the splitting strength decreases with porosity following an exponential decay. A similar trend is observed experimentally in recent studies a model gypsum plaster material [44].

5. Conclusion

In summary, a framework for fabricating and testing of cement paste micro-cubes was designed. Based on an analogy with Brazilian splitting test, nominal splitting tensile strength was derived from the measured maximum load. To deal with the heterogeneity of this material at micro metre scale, large amount of data was obtained from specimens with different w/c ratios and analysed using Weibull statistics. The experimentally measured splitting tensile strength fills the gap between meso scale and nano scale. In parallel with the experiments, the fracture performance of micro-cubes under the indentation splitting was simulated using the microstructure informed lattice fracture model, and a good agreement was found between the simulation and experiment except the post-peak results which cannot be captured experimentally due to the instrumental limitation. The following conclusions can be

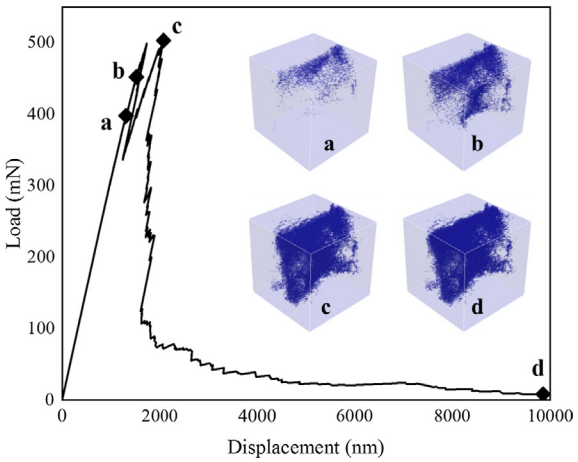

Fig. 16. Simulated fracture patterns of micro-cube (considering the adhesive-layer) under different loading state: (a) initial state which has 5000 broken elements with a response of 398 mN of load and 1.3 μm of indentation depth; (b) crack pattern with 20,000 broken elements, 1.7 μm indentation depth, and responses for 452 mN (c) crack pattern at peak load of 503 mN with 44,988 broken elements under indentation depth of 2.1 μm (d) failure state at indentation depth of 10 μm with 50,780 broken elements.

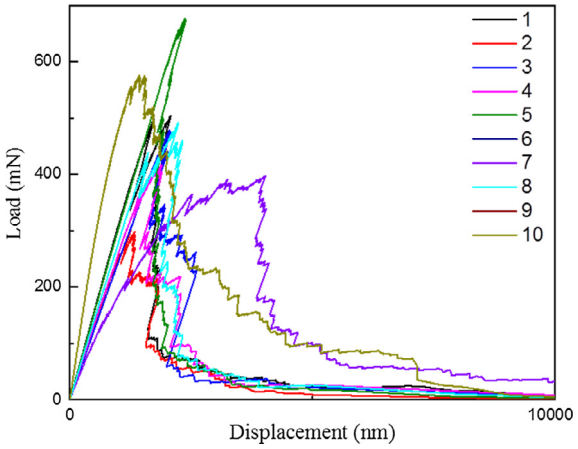

Fig. 17. Simulated load-displacement curve of micro-cubes under indentation splitting.

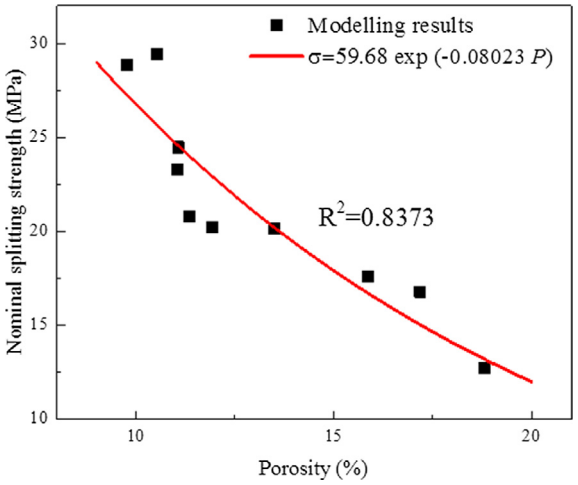

Fig. 18. Relationship between nominal splitting strength and porosity from the simulation.

drawn:

The tensile strength of cement paste at micro scale was found to be an order of magnitude lower than the values of individual cement hydrated phases, but an order of magnitude higher than the macroscopic values of cement paste or concrete.

The influence of initial w/c ratio of mixture on the nominal splitting strength was studied and it is found that with an increasing w/c ratio, the micro scale specimens are more likely to yield a lower strength and have a higher dispersion.

Since the measured displacements also include deformation of the supporting adhesive-layer and local imprinting of the indenter into the micro-cube, the stiffness or modulus of tested micro-cubes cannot directly be obtained from the recorded load-displacement curves, further investigations are expected to solve this limitation. Furthermore, a nano-indenter with higher load capacity is suggested for the materials with stronger microstructures.

The recorded load-displacement curve was successfully used as a validation for the micro scale fracture modelling. Together with the method presented in [21] the framework for fitting and validation of the modelling results at micro scale is created. This method forms also a basis for validation of multi-scale modelling results at every scale.

Acknowledgements

This work was supported in part by the scholarship from China Scholarship Council. Additionally, the authors would like to acknowledge the help of Arjan Thijssen with SEM experiments.

Appendix A. Appendix A

Herein, a two-component epoxy adhesive (Araldite 2020) was adopted for bonding glass substrate and cement for micro-cube fabrication. In order to get the micromechanical properties of the adhesive as input for fracture simulation, grid nanoindentation tests were performed. The two components were mixed uniformly and dropped on the glass substrate to form a hardened film with a thickness of around 1 mm. Prior to testing, the adhesive film was ground using sandpaper to reach a relative flat and smooth surface. After grinding, the film was polished with 6 μm (5 min), 3 μm (5 min), 1 μm (10 min), and 0.25 μm (30 min) diamond paste on a lapping table. Each suspension was used for 30 min and after each polishing step, samples were soaked into an ultrasonic bath to remove any residue.

A series of 10 × 10 indents was performed on the polished surface with a spacing of 20 μm between each indent using the Agilent Nanoindenter G200 (Keysight, Santa Rosa, CA, USA) equipped with a diamond Berkovich tip. The Continuous Stiffness Method (CSM) proposed by Oliver and Pharr [45], which provides continuous measurements of elastic modulus as a function of indentation depth, was used to analyse the results. Indentation depth was set to 1000 nm and the average E modulus was determined in the loading range between 800 and 900 nm. For the calculation, Poisson's ratio of the indented material was estimated as 0.3. An average value of 3.06 MPa with a standard deviation of 0.42 MPa was derived from 100 indents indicating that a deterministic value can be used for the simulation. As the adhesive element in the simulation is not allowed to fail, it has no contribution to the predicted strength in the modelling. Therefore, there is no demand for the strength of this element in the simulation.

Appendix B. Supplementary material

Supplementary data associated with this article can be found, in the online version, at http://dx.doi.org/10.1016/j.engfracmech.2018.04.018.

Reference

[1] Van Mier JG. Concrete fracture: a multiscale approach: CRC Press; 2012.
[2] Bernard O, Ulm F-J, Lemarchand E. A multiscale micromechanics-hydration model for the early-age elastic properties of cement-based materials. Cem Concr Res. 2003;33:1293–309.
[3] Hlobil M, Šmilauer V, Chanvillard G. Micromechanical multiscale fracture model for compressive strength of blended cement pastes. Cem Concr Res. 2016;83:188–202.
[4] Qian Z. Multiscale modeling of fracture processes in cementitious materials [PhD. Thesis]. Delft, The Netherlands: Delft University of Technology; 2012.
[5] Vorel J, Šmilauer V, Bittnar Z. Multiscale simulations of concrete mechanical tests. J Comput Appl Mathemat 2012;236:4882–92.
[6] Pichler B, Hellmich C. Upscaling quasi-brittle strength of cement paste and mortar: A multi-scale engineering mechanics model. Cem Concr Res 2011;41:467–76.
[7] Tennis PD, Jennings HM. A model for two types of calcium silicate hydrate in the microstructure of Portland cement pastes. Cem Concr Res 2000;30:855–63.
[8] Pellenq RJ-M, Kushima A, Shahsavari R, Van Vliet KJ, Buehler MJ, Yip S, et al. A realistic molecular model of cement hydrates. Proceedings of the National Academy of Sciences. 2009;106:16102–7.
[9] Němeček J, Králík V, Šmilauer V, Polívka L, Jäger A. Tensile strength of hydrated cement paste phases assessed by micro-bending tests and nanoindentation. Cem Concr Compos 2016;73:164–73.
[10] Constantinides G, Ulm F-J. The effect of two types of CSH on the elasticity of cement-based materials: results from nanoindentation and micromechanical modeling. Cem Concr Res 2004;34:67–80.
[11] Sanahuja J, Dormieux L, Chanvillard G. Modelling elasticity of a hydrating cement paste. Cem Concr Res 2007;37:1427–39.
[12] Zhang M, Jivkov AP. Micromechanical modelling of deformation and fracture of hydrating cement paste using X-ray computed tomography characterisation. Composites Part B: Eng 2016;88:64–72.
[13] Luković M, Schlangen E, Ye G. Combined experimental and numerical study of fracture behaviour of cement paste at the microlevel. Cem Concr Res 2015;73:123–35.
[14] Pichler B, Hellmich C, Eberhardsteiner J, Wasserbauer J, Termkhajornkit P, Barbarulo R, et al. Effect of gel–space ratio and microstructure on strength of hydrating cementitious materials: an engineering micromechanics approach. Cem Concr Res 2013;45:55–68.
[15] Zhang H, Šavija B, Figueiredo SC, Schlangen E. Experimentally validated multi-scale modelling scheme of deformation and fracture of cement paste. Cem Concr

Res 2017;102:175–86.
[16] Van Breugel K. Numerical simulation of hydration and microstructural development in hardening cement-based materials:(II) applications. Cem Concr Res 1995;25:522–30.
[17] Bentz DP. Three-Dimensional Computer Simulation of Portland Cement Hydration and Microstructure Development. J Am Ceramic Soc 1997;80:3–21.
[18] Bishnoi S, Scrivener KL. μic: a new platform for modelling the hydration of cements. Cem Concr Res 2009;39:266–74.
[19] Scrivener KL. Backscattered electron imaging of cementitious microstructures: understanding and quantification. Cem Concr Compos 2004;26:935–45.
[20] Gallucci E, Scrivener K, Groso A, Stampanoni M, Margaritondo G. 3D experimental investigation of the microstructure of cement pastes using synchrotron X-ray microtomography (μCT). Cem Concr Res 2007;37:360–8.
[21] Zhang H, Šavija B, Chaves Figueiredo S, Lukovic M, Schlangen E. Microscale testing and modelling of cement paste as basis for multi-scale modelling. Materials 2016;9:907.
[22] Chen SJ, Duan WH, Li ZJ, Sui TB. New approach for characterisation of mechanical properties of cement paste at micrometre scale. Mater Design 2015;87:992–5.
[23] Liu D, Flewitt PE. Deformation and fracture of carbonaceous materials using in situ micro-mechanical testing. Carbon 2017;114:261–74.
[24] Šavija B, Liu D, Smith G, Hallam KR, Schlangen E, Flewitt PE. Experimentally informed multi-scale modelling of mechanical properties of quasi-brittle nuclear graphite. Eng Fract Mech 2016;153:360–77.
[25] Zhang J, Scherer GW. Comparison of methods for arresting hydration of cement. Cem Concr Res 2011;41:1024–36.
[26] Li X, Bhushan B. A review of nanoindentation continuous stiffness measurement technique and its applications. Mater Characterizat 2002;48:11–36.
[27] Rocco C, Guinea GV, Planas J, Elices M. Size effect and boundary conditions in the Brazilian test: experimental verification. Mater Struct 1999;32:210–7.
[28] Nilsson S. The tensile strength of concrete determined by splitting tests on cubes. RILEM Bulletin 1961;11:63–7.
[29] Zhang M, He Y, Ye G, Lange DA, van Breugel K. Computational investigation on mass diffusivity in Portland cement paste based on X-ray computed micro-tomography (μCT) image. Constr Build Mater 2012;27:472–81.
[30] Zhang M, Jivkov AP. Microstructure-informed modelling of damage evolution in cement paste. Constr Build Mater 2014;66:731–42.
[31] Schlangen E. Crack development in concrete, part 2: modelling of fracture process. Key Eng Mater: Trans Tech Publ; 2008. p. 73-6.
[32] Šavija B, Smith GE, Heard PJ, Sarakinou E, Darnbrough JE, Hallam KR, et al. Modelling deformation and fracture of Gilsocarbon graphite subject to service environments. JNuM. 2017.
[33] Yip M, Mohle J, Bolander J. Automated modeling of three-dimensional structural components using irregular lattices. Comput-Aided Civil Infrastruct Eng 2005;20:393–407.
[34] Lilliu G. 3D analysis of fracture processes in concrete: Eburon Uitgeverij BV; 2007.
[35] Hu C, Li Z. Micromechanical investigation of Portland cement paste. Constr Build Mater 2014;71:44–52.
[36] Velez K, Maximilien S, Damidot D, Fantozzi G, Sorrentino F. Determination by nanoindentation of elastic modulus and hardness of pure constituents of Portland cement clinker. Cem Concr Res 2001;31:555–61.
[37] Gao Y, Zhang Y, Hu C, Li Z. Nanomechanical properties of individual phases in cement mortar analyzed using nanoindentation coupled with scanning electron microscopy. J Chinese Ceramic Soc 2012;40:1559–63.
[38] Pizette P, Martin C, Delette G, Sornay P, Sans F. Compaction of aggregated ceramic powders: From contact laws to fracture and yield surfaces. Powder Technol 2010;198:240–50.
[39] Odler I, Rößler M. Investigations on the relationship between porosity, structure and strength of hydrated Portland cement pastes. II. Effect of pore structure and of degree of hydration. Cem Concr Res 1985;15:401–10.
[40] Kumar R, Bhattacharjee B. Porosity, pore size distribution and in situ strength of concrete. Cem Concr Res 2003;33:155–64.
[41] Bažant ZP. Size effect in blunt fracture: concrete, rock, metal. J Eng Mech 1984;110:518–35.
[42] Eliáš J, Vořechovský M, Skoček J, Bažant ZP. Stochastic discrete meso-scale simulations of concrete fracture: comparison to experimental data. Eng Fract Mech 2015;135:1–16.
[43] Salviato M, Chau VT, Li W, Bažant ZP, Cusatis G. Direct testing of gradual postpeak softening of fracture specimens of fiber composites stabilized by enhanced grip stiffness and mass. J Appl Mech 2016;83:111003.
[44] Liu D, Šavija B, Smith GE, Flewitt PE, Lowe T, Schlangen E. Towards understanding the influence of porosity on mechanical and fracture behaviour of quasi-brittle materials: experiments and modelling. Internat J Fract 2017;1–16.
[45] Oliver WC, Pharr GM. Measurement of hardness and elastic modulus by instrumented indentation: Advances in understanding and refinements to methodology. J Mater Res 2004;19:3–20.